Tunable H-alpha Lyot filter with advanced servo system and image processing: instrument design and new scientific results with the Dutch Open Telescope

SPIE vol. 6269, *Ground-based and Airborne Instrumentation for Astronomy*, paper 12, 2006

Felix C.M. Bettonvil[*a,b], Robert H. Hammerschlag[a], Peter Sütterlin[a,b],
Robert J. Rutten[a], Aswin P.L. Jägers[c], Guus Sliepen[a]
[a]Astronomical Institute, Utrecht University, The Netherlands;
[b]Netherlands Foundation for Research in Astronomy ASTRON, Dwingeloo, The Netherlands;
[c]Physics Instrumental Group IGF, Utrecht University, The Netherlands

ABSTRACT

The Dutch Open Telescope (DOT; `http://dot.astro.uu.nl`) on La Palma is a revolutionary open solar telescope, on an excellent site, on top of a transparent tower of steel framework, and uses natural air flow to minimize local seeing. The DOT is a high-resolution multi-wavelength imager capable of long-duration time series aiming at magnetic fine structure, topology and dynamics in the photosphere and low- and high chromosphere. In this paper we describe the latest addition to the multi-wavelength imaging system: a Lyot H-alpha camera channel operating at a wavelength of 656.3 nm, being of major interest for high-chromospheric phenomena. The channel is operated strictly synchronous with the other channels and all data are speckle reconstructed. The channel permits profile sampling and delivers Dopplergrams in a 15 second time cadence, up to several hours long and adding up to a total data amount of 1.6 Terabyte/day. A dedicated computer (DSP, DOT Speckle Processor) has been built for processing the data overnight.

Keywords: solar telescopes, telescope optics, diffraction limited imaging, speckle masking, seeing, wind, H-alpha, Lyot filter, tomography, magneto-hydrodynamics

1. INTRODUCTION

1.1 Dutch Open Telescope

The Dutch Open Telescope (DOT), shown in Figure 2 (left) and located at the Observatorio del Roque de los Muchachos on La Palma is at the forefront of high-resolution solar observations. It became the first solar telescope to regularly achieve images with 0.2" resolution continuously over multiple hours and large fields (80"x60") at high cadence (30 s) thanks to its successful open principle, superb optical performance, exceptional mechanical stability and the homogeneous wind flows which make La Palma a world-class site [1-5]. Figure 1 shows an example of a typical image sequence taken with the DOT. All DOT data are downloadable from the DOT-website `http://dot.astro.uu.nl`, thanks to the DOT open data policy [1].

Both the telescope and tower are open, i.e. transparent for the wind. The DOT consists of a 15 m high open framework tower and a dome-less telescope. Already when there is a light breeze it limits the solar heated boundary layer of turbulent convection to heights below the telescope and flushes both telescope and tower, keeping the air temperature homogeneous. Warm air bubbles are not forced upwards against solid walls and no heat is produced by the tower itself. The tower and telescope must be extraordinarily stiff to avoid image shake from wind buffeting but at the same time be transparent for the wind. The tower consists of parallel triangles minimizing rotations around all axes. Details about the design are given in [2, 4]. The telescope is equatorial, built very compact and rigidly, with the primary mirror lifted above the declination axis during observations, with the complete optical light path being above the telescope, in order to be

[*] F.C.M.Bettonvil@astro.uu.nl; phone +31 30 2535218/2535200; fax +31 30 2535201; http://dot.astro.uu.nl; Astronomical Institute, Utrecht University, Princetonplein 5, NL-3584 CC Utrecht, The Netherlands

fully exposed to the natural wind flow. The mount contains a novel drive system combining high stiffness with minimal friction and stick-slip [2, 3, 4, 6].

The open concept was new, because all existing high-resolution solar telescopes use evacuation to avoid internal turbulence. The DOT has a modest size, but its successful demonstration of the open principle and its ability to be up-scaled towards much larger apertures (no need for lenses or windows to close the vacuum tank), together with the rapid development of adaptive optics in solar imaging, started a new age in solar telescope engineering with GREGOR [7], ATST [8], the plan for a DOT-upgrade to 1.4 m [9] and large open tower designs [10, 11, 12] being good examples.

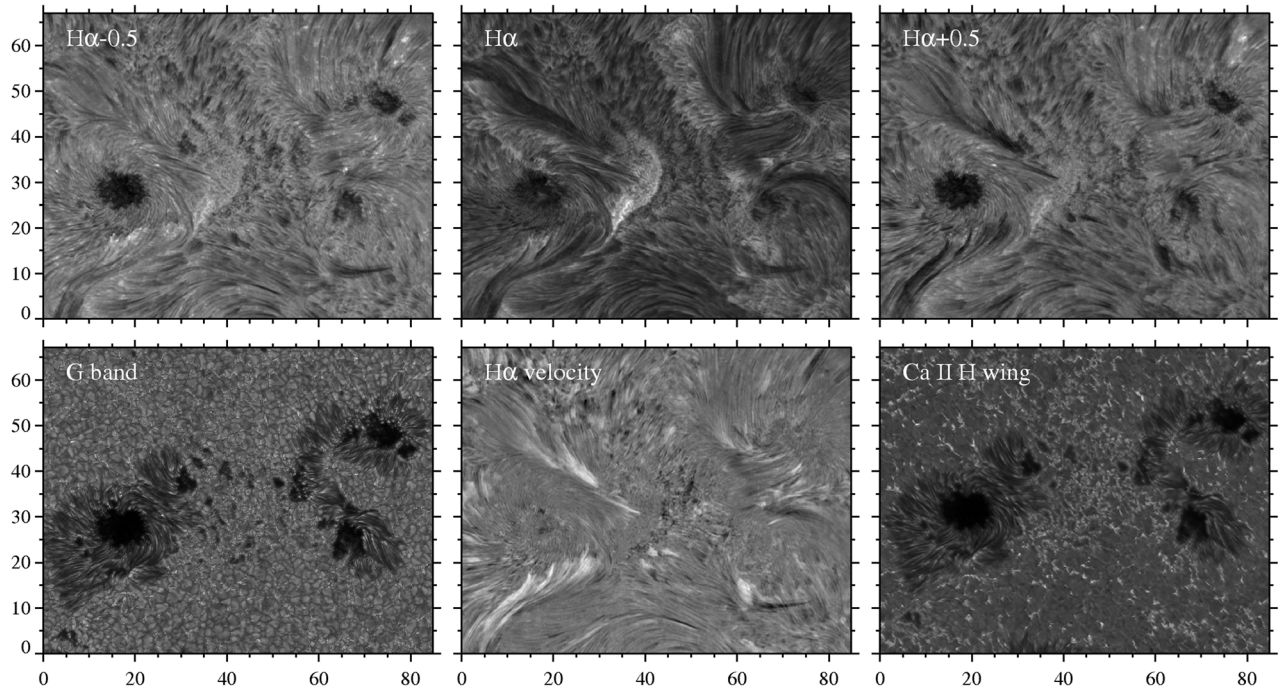

Fig. 1. A snapshot of a two-hour multi-channel sequence taken with the DOT. It shows the bipolar spot region NOAA 10786 on July 9, 2005 at 8:50 UT, observed in the context of International Time Program campaign led by Y. Katsukawa. The top row displays three narrow-band filtergrams, in the core of the Balmer H-alpha line (middle image) and the two wings. The line originates in the high chromosphere of the sun, a region some 1500 km above the photosphere that is filled with loops of magnetic field lines. The bright, thread-like area in the core image is a micro-flare, the release of energy due to reconfiguration of the magnetic field lines. The left image is a slightly blue shifted wing image and here a dark area is due to lower temperature (umbra of the sunspot) or due to upward mass motion (dark streak in the lower right of the field of view). By combining the two wing images it is possible to compute velocities within this part of the atmosphere - this Dopplermap is shown in the middle image in the lower row. White areas show matter that is moving away from the observer, dark areas matter that moves towards us. In some areas loop flows can be seen: arcs that are white on one end and black on the other.

The lower left image shows the photosphere of the sun, the height where most of the visible light of the sun originates. Outside the spots, it shows granulation. It is taken in the Fraunhofer G band, a region of the solar spectrum filled with many molecular absorption lines of CH. The tiny bright points are flux tubes, magnetic concentrations and the foot points of the loops seen in the H-alpha images. The smallest details visible have a resolution of 0.2", corresponding to 140 km. The lower right image is taken in the wing of the H-line of singly ionized calcium, the strongest line in the solar spectrum. It probes a height some 400 km above the photosphere where the convection has already vanished (i.e. the flat appearance of the areas covered by granulation in the G-band image) but the magnetic flux tubes can still be seen as white dots or crinkles. Every multi-channel sequence includes a blue- and red continuum image too, not displayed here. For more DOT images and movies see the DOT-website `http://dot.astro.uu.nl`.

1.2 Optical configuration

The DOT optics, described in detail in [3] and schematically shown in Figure 2, consist of a 450mm F/4.44 parabolic mirror with behind the primary focus a lens system which enlarges the primary image 10x and which compensates for coma (as introduced by the parabolic primary). In the primary focus a reflective and water-cooled field-stop is located. Behind the enlargement system a beam-splitter is mounted, splitting up the light between the on-axis G-band camera

(430.5 nm) and 5 other cameras, mounted on the side of the telescope top. All cameras together form a multi-wavelength imaging system. The cameras observe in the above mentioned G-band, two continuum channels (432 and 655 nm) and Ca II H (396.8 nm). Recently H-alpha (656.3 nm), being the topic of this paper, is added and soon Ba-II (455.4nm) will follow [1, 3, 13]. The channels are fed by dichroic splitters and all optical components are diffraction limited and precisely aligned. The enlargement lens is minimized for spherical aberration at 430.5 nm (G-band), however introduces spherochromatism at other wavelengths due to the high F-ratio. This is corrected within each camera channel separately by use of meniscus lenses. A detailed drawing of the complete multi-wavelength-system is printed in [3].

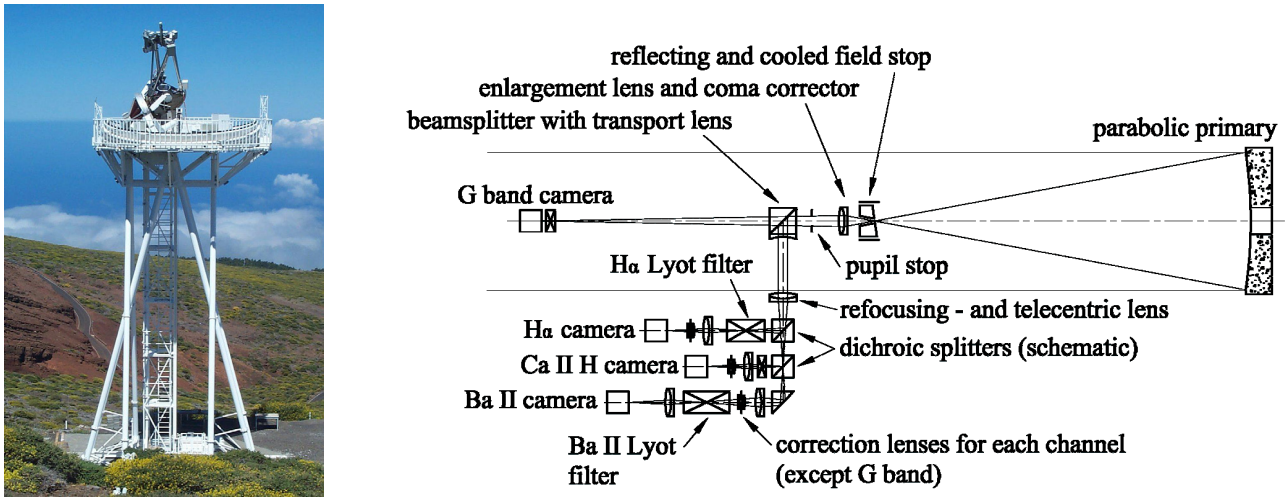

Fig. 2. *(left)* The Dutch Open Telescope (DOT) on La Palma, observing the sun; *(right)* optics sketch of the DOT optical layout. The multi-wavelength imaging system is visible below the primary beam and simplified for clarity. The two continuum channels have been neglected and in reality the dichroic splitters are not cubes but mirrors reflecting on a small angle. The complete multi-wavelength imaging system is mounted in the top of the telescope, see also Figure 5.

The present DOT camera field measures 116" over the diagonal, as determined by the effective focal length (19.75 m) and CCD dimensions. The maximum field for the DOT and multi-wavelength system is currently 2.7 arcminutes and at maximum 4 arcminutes, as set by the maximum field of view of the coma corrector and filter apertures.
All channels use Hitachi KP-F100 cameras (1296x1030 pixels, 6.7 μm^2, max. 12 frames/sec) and work strictly synchronously. They transmit their images to an acquisition computer, accommodating 1.6 Terabyte of storage capacity, in standard mode sufficient for 8-hour runs.

1.3 Image reconstruction

The DOT does not rely on Adaptive Optics, but instead uses purely the speckle reconstruction technique for restoring the image from atmospheric turbulence [1, 13, 14]. Speckle has been chosen because it delivers good and consistent restoration over the whole field of view and excellent temporal sequence homogeneity, despite its disadvantage of laborious post-detection processing. For obtaining one corrected image, the technique requires a speckle burst of 100 frames within 15 to 30 seconds (in order to avoid smearing by solar motion itself) with exposure times below the seeing-freezing time of 20 ms, forming an independent set of samples of the wave-front distortions. The full field of view is tessellated into about a thousand subfields, each smaller than the iso-planatic patch over which the atmospheric wave-front perturbations do not vary with angle. For each subfield the speckle reconstruction is done independently using all burst frames which then are merged into a single sharp image. Nearly diffraction-limited resolution over the whole field of view is reached on days with Fried parameters of only 7 cm, which occurs fairly frequently on La Palma. The resulting DOT movies are well-known and when the La Palma seeing is good enough an entire multi-hour image sequence consistently possesses diffraction-limited resolution.

2. H-ALPHA CHANNEL

2.1 Introduction

The H-alpha channel is the most recently installed addition to the multi-wavelength imaging system. It images the Balmer H-alpha line at 656.3 nm which shows the higher part of the chromosphere. One goal is to make Doppler movies, image sequences which show velocity information in the line of sight. For Doppler information it is needed to make images in both wings of the line and for this the filter should be tunable. In order to avoid smearing due to motion of structures in the solar atmosphere, both images should be taken within the 15-30 seconds cadence time. The splitting up of the speckle burst in sub-bursts complicates speckle reconstruction and to overcome this we make use of the narrow/broad band speckle reconstruction method as described by Keller & Von der Lühe [14]. They use a nearby broad band channel to reconstruct the narrow channel. Originally the method was invented to improve signal-to-noise in single narrow band images, but works well in case of reconstructing sub-bursts. In addition, because of the rapidly changing appearance of H-alpha images with wavelength, the broad-band channel serves in aligning successive images.
H-alpha images show intensity variations due to different physical processes, see Section 4, and in order to disentangle them it is necessary to perform full profile modeling. For this reason one H-alpha burst is not only split up in two wing images, as needed for a Dopplergram, but divided in up to 5-7 sub-bursts on different wavelengths in the H-alpha line.

2.2 H-alpha filter

For the tunable H-alpha filter we make use of a Lyot filter. The Lyot filter, as invented by Bernard Lyot [15] and in detail described in later papers by Lyot [16] and Evans [17], is a type of optical filter that uses birefringence to produce a narrow pass-band. Particularly in solar astronomy Lyot filters are well-known. There exist several types of birefringent filters differing in field of view and complexity. In its most basic form, light traveling through a birefringent plate is split into two rays (respectively the ordinary and extraordinary rays), each experiencing a different refractive index and thus having a different phase velocity. Only wavelengths at which the ordinary and extraordinary rays have optical path lengths equal to an integer multiple of the wavelength exit the plate in the same polarization state as they entered the plates. Polarizers at the front and at the back of the birefringent plate produce a filter with a sinusoidal transmission function. The wavelength interval between successive peaks is inversely proportional to the thickness of the plate. Adding more plates -each next one has double the thickness of the previous one- narrows the main peak. The bandwidth of the total filter is set by the thickest plate whereas the distance between successive peaks is set by the thinnest one. Adding waveplates and rotating the stages (with help of a gear-box, in order to rotate the stage of a thicker plate double as fast as the preceding plate) shifts the wavelength of the transmission peaks over the same amount, allowing the filter to be tuned. Advantage of a birefringent filter is the wide field of view, i.e. a low wavelength shift as function of the entrance angle of the incident ray, compared to Fabry-Perots and etalons [18]. Lyot-filters can be tuned quickly, but have a relative low transmittance. For the narrow/broad band speckle reconstruction this turns out however not be a drawback.

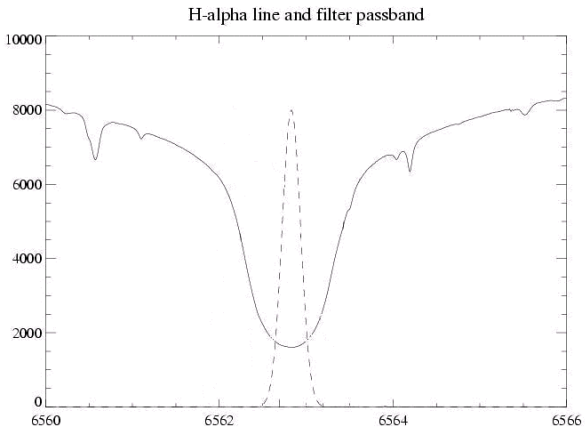

Fig. 3. The H-alpha absorption line in the solar spectrum and 0.025 nm pass-band of the Zeiss H-alpha filter (dashed line).

For the DOT H-alpha channel a simple Lyot-Öhmann type H-alpha filter (656.3nm) from Zeiss, Germany has been modernized. It was used for many years at the Ottawa River Solar Observatory and made available to us by Gaizauskas [19]. The filter is tunable and has a selectable pass-band of 0.025 or 0.050 nm (FWHM). The light passing through the filter is plane polarized in a vertical plane. Figure 3 shows the pass-band in proportion to the H-alpha profile.
Temperature dependence is a critical property for birefringent crystals. Both its geometrical dimensions and retardation characteristics are temperature dependent and it results in a shift in wavelength of the transmission pass-band. For quartz the dependence is in the order of -0.066 nm/°K at red wavelengths. The temperature of a Lyot-filter should be kept stable

within a few hundreds of a degree centigrade. For this reason the filter is surrounded by a heating spiral and has additional heating elements at the front- and back ends, with 100 W electrical power in total and is heated to 45˚C. It ensures a homogeneous temperature. A servo amplifier keeps the temperature stable within a few 1/100˚C. Because the polarizers in the Lyot filter are cemented and hence sensitive to breakage at low temperatures, special care is needed during winter time in avoiding power cuts.
The filter allows for a beam divergence of ±1.6˚ for the pass-band of 0.025 nm and ±2.5˚ for the pass-band of 0.050 nm. The overall optical length is 258 mm. The clear aperture of the entrance window measures 36 mm; the exit window is 26 mm in diameter. All optical components are immersed in silicone oil with an index of refraction close to that of the crystals in order to reduce reflections. Glass-to-air surfaces are coated for a wavelength of 656.3 nm.
The first component is a multi-layer interference filter, which is a heat rejection filter in addition. After the interference filter the light beam passes through the first polarizer. The Zeiss Lyot filter contains three groups of birefringent quartz crystals and five groups of calcite crystals. All are cut parallel to their principal optic axis. The thickest elements are split and provided with a λ/2-plate, giving the filter a wider field. The thinner quartz plates are combined with the calcite plates in groups, as described by Evans [17], in order to save polarizers which improves the throughput.
Switching between 0.025 and 0.050 nm is done by adding or removing the last polarizer, making the thickest calcite element active respectively inactive. When taken out, the polarizer is replaced by a glass plate to maintain focus position. The total wavelength tuning range is ± 1.6 nm, with 656.3 nm as the central wavelength. The distance between successive peaks is 12.8 nm.

2.3 H-alpha optics

As described in sub-section 2.1, the H-alpha channel consists of 2 camera channels: the narrow-band Lyot-channel and a broader continuum channel. The continuum wavelength is 655.05 nm (FWHM 0.25 nm) and is chosen close to the H-alpha line in a spectral range in the solar spectrum with absence of other absorption lines. The continuum filter can be replaced by an H-alpha interference filter (656.28 nm, FWHM 0.25 nm), being 10 times broader than the Lyot-channel and well suited for prominence observations. Both filters are made by Barr Associates Inc., Westford, MA, USA with precisely the correct center wavelength for perpendicular light transmission. Tilting substantially the filters for tuning would influence negatively the spatial telescope resolution because of asymmetric apodisation effects in the pupil.
Figure 4 shows the layout of the channel. The dichroic split unit, described in more detail in [3], is fed by the telescope optics and distributes the light to the camera channels (except for the G-band camera which is mounted on-axis and already split-off before the dichroic split unit). It consists of dichroic mirrors reflecting on small angles (8˚) and divides the beam in a violet (380–400 nm), blue (410–510 nm) and red part (580-800 nm). The red beam feeds the two H-alpha channels. Splitting between the two H-alpha channels is done with a broad-band polarizing cube beam-splitter (wavelength range 450-680 nm). The reflected beam is directed to the Lyot channel; the transmitted beam feeds the continuum channel. The Lyot-filter is oriented such that entrance polarization of the filter coincides precisely with the direction of polarization of the beam-splitter. In this whole region the beam is telecentric, which is of importance for filters as it ensures that any image point in the field of view possesses identical filter characteristics.
We continue with a description of the Lyot channel. The first component is an interference filter. The original Zeiss pre-filters has been taken out (which were integrated in the Lyot filter) and replaced by an external narrow band 1.5 nm interference filter also from Barr. It is mounted in front of the Lyot filter.
Inside the H-alpha filter an intermediate image is formed. Doing so leads to an optical design which uses the smallest possible beam diameter. Our experience is that avoiding the use of the outer part of any aperture gives better optical performance. Behind the Lyot filter two achromats (both with f = 450 mm, standard from LINOS, interferometrically tested and selected from a large sample) in tandem act as a re-imaging lens and produce a 1:1 image to the camera. Between these lenses and the camera a pupil image is located and at this place meniscus lenses are mounted which shift the wavelength of minimum spherical aberration from the Fraunhofer G-band (430.5 nm) towards H-alpha, as mentioned in sub-section 1.2. Such a correction is done for all camera channels (except G-band) as illustrated in Figure 2 and described by Bettonvil in [3].
The continuum channel is, apart from the thick Lyot-filter, optically identical with the Lyot-channel. Next to the H-alpha channels a third channel is implemented (not shown in Figure 4) which is connected to H-alpha observations too. It is a wide field camera equipped with a commercial H-alpha filter (Solarcope 50, Solarscope Ltd, UK) providing a full disk image. It assists in monitoring filaments and prominences.

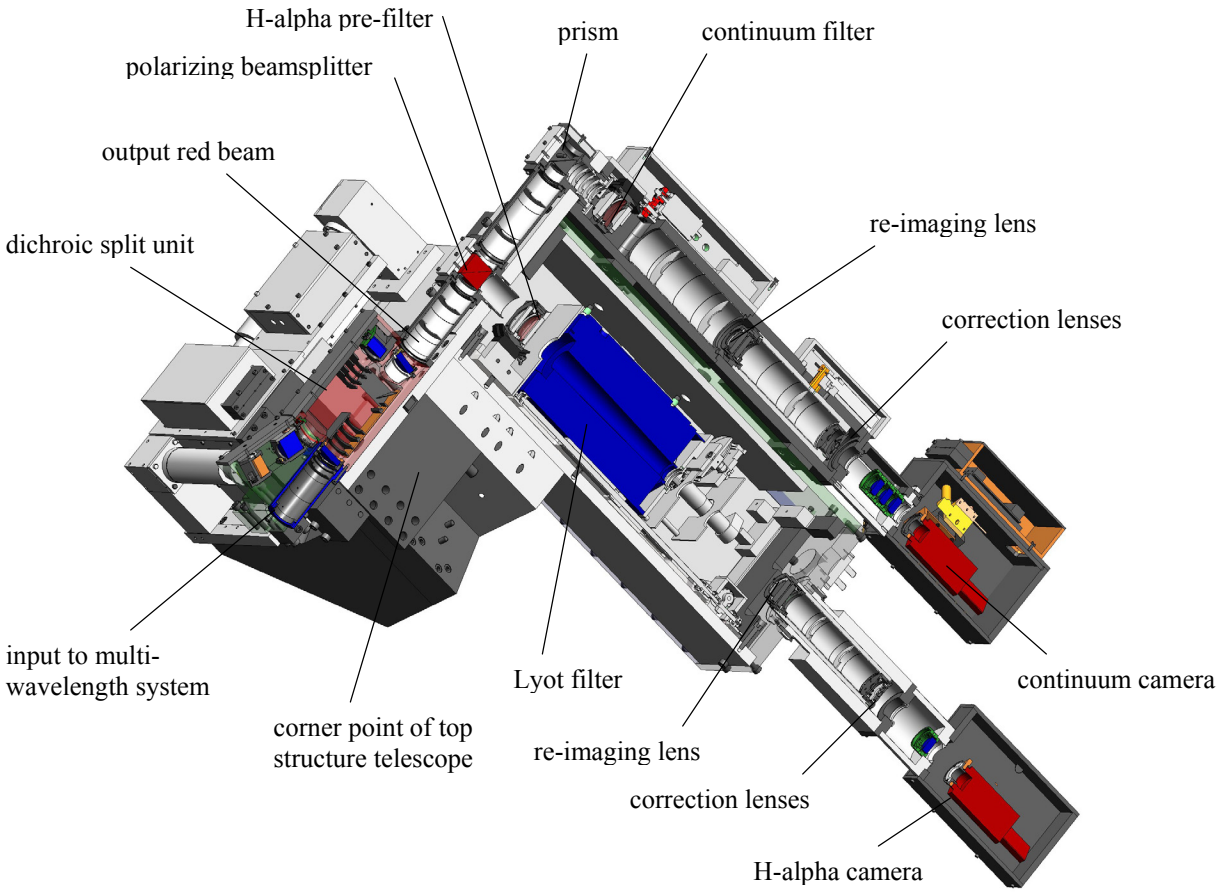

Fig. 4. Cross section of the H-alpha channel together with the dichroic splitter unit.

2.4 Mechanical design

The filter measures 306x150x150 mm. It is housed in a metal box-shaped structure, see Figure 4, manufactured from aluminum plate, with thicknesses ranging from 18 to 30 mm, and bolted together. The box forms the stiff base for filter, optics and camera and is connected to one of the three corner points of the top of the telescope. Big stiffness is a major design criterion: the channel (together with all other channels of the multi-wavelength imaging system) moves during an observing day from eastern horizon through approximately zenith towards western horizon and should be stiff against wind gusts, just like tower and telescope. All CCDs should keep their alignment within a few 0.01 mm. The box is attached to the telescope such that a fixed reference point exists: parts of the structure can slightly lengthen and shorten due to temperature differences without the occurrence of creep on the long term. Stick-slip between construction parts is minimized through a thin layer of grease (DX from Molykote, a division of Dow Corning).
For the Lyot-filter with its multiple rotating stages, stability in terms of wavelength setting and mechanical stability of the optical components under the changing gravity load is another important requirement. It has been tested and we didn't see any degradation in image quality, shifts of optical components or change in wavelength setting due to the change of filter orientation.
The inside walls of the box are insulated with 10mm neoprene cell rubber. It prevents for heat leaking to ambient and possible negative impacts on telescope seeing. The neoprene rubber is black and acts as stray light protection too.
The Lyot-filter is mounted on a translation stage -using pre-loaded Schneeberger linear crossed roller bearings- which allows for translation along the optical axis. It is used to prevent that the intermediate focal plane in the filter is located close to an optical surface and introduces optical imperfections in the camera image. The adapter plate between filter and

translation stage is made of Celeron (synthetic resin bonded fabric made of phenolphormaldehide and cotton), which combines relatively large stiffness (E-modulus 7.10^{9} N/m^{2}), a linear coefficient of thermal expansion similar to metal (2.10^{-05} K^{-1}), with a low coefficient of thermal conductivity (2.10^{-1} W/m˚K).
At the exit side of the box an extension tube is mounted accommodating the re-imaging lens, correction lenses and camera house. Both box and tube are baffled with stray-light baffles keeping stray-light below the camera noise level. The baffles are made of aluminum, sand-blasted and black anodized.
The lens mounts are designed such that minimal stress and no bending force is applied to the lenses, which avoids the introduction of aberrations. The lenses are fixed on three points confining the radial and axial position. The lenses are kept in position by tiny springs applying only slightly more force than the weight of the lens. The combination of lens and mount has been tested on an interferometer and didn't show measurable wave-front distortions ($<\lambda/10$).
The camera is mounted on a combined xyz-/gonio-stage which allows for focusing and image alignment with the other cameras. Figure 5 shows the H-alpha channel mounted on the DOT.

Lyot filters are known for their sensitivity to jerks, which can disorientate the positions of the crystal plates. The wavelength tuning is done by rotating the crystal plates around the optical axis with a gearbox connected to a modern servomotor system based on a Maxon DC servo-motor (precious metal brush type, 10 W) with optical encoder (500 counts/rev., differential quadrature with index pulse). One thousand counts do equal 0.025 nm in bandwidth.
Two extra motors are used to translate the Lyot filter and for selection of the bandwidth (0.025 or 0.050 nm). Elimination of vibrations and jerks is reached by S-curve control (see sub-section 2.5) and precise mechanical design and fabrication. The motor system has limit switches which limit the total travel range and an additional safety switch which disables the servo-amplifiers giving maximum protection in case of a fault in the servo system/software, hence position loss and disorientation of the crystal plates are well secured.

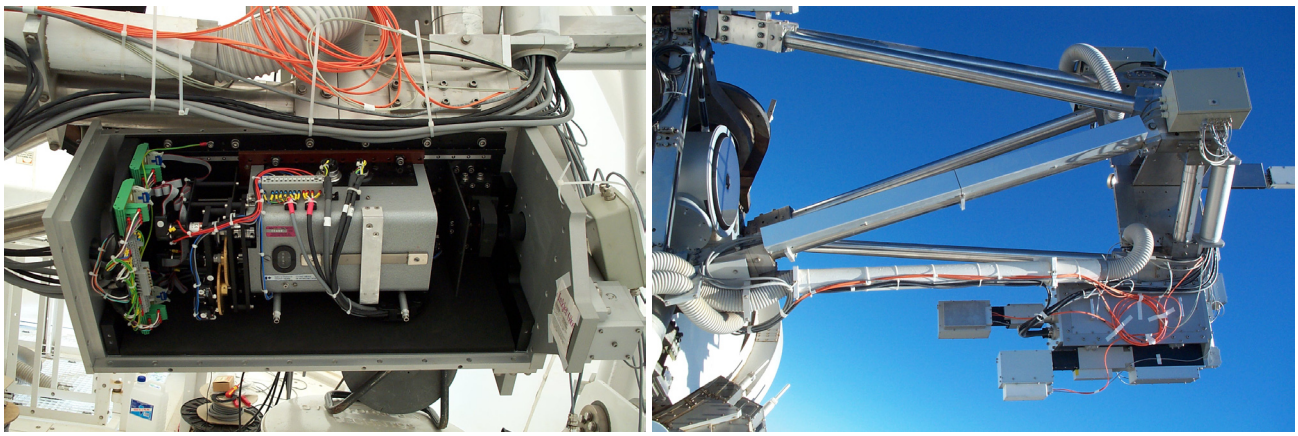

Fig. 5. *(left)* Dutch Open Telescope with opened H-alpha channel. The grey box in the center is the Lyot filter; at the left the servo motor and gear system is visible. At the right in the black area the pre-filter is mounted. The light enters the box from the right, and leaves the box at the left side to the camera. The camera is not mounted yet; *(right)* top of the telescope with below the two H-alpha channels, the upper one being the Lyot-, the lower one the continuum channel. At the left the primary mirror is visible.

2.5 Control

The servo motors are controlled with a Halbeck POSYS 804 PID motion controller. It can control up to four axes and runs on a Linux OS. The card is PC/104 compliant and fits on a WinSystems PPM-520 mini-PC which handles all control signals to the different servo motors of the DOT multi-wavelength imaging system and is mounted nearby the camera channels in the top of the telescope. The motion controller feeds Maxon analogue servo amplifiers which power the motors. Analogue technology is chosen in order to guarantee smooth movement and minimize the risk of electromagnetic interference to the camera signals.
Optimum control parameters are set using the method of Ziegler and Nichols, based on information of the ultimate gain and ultimate oscillation frequency. It combines a minimal static error and a fast response with roughly 25% overshoot. The Halbeck controller enables the use of a S-curve motion generator, giving the possibility to program the derivative of the acceleration, known as jerk. It realizes a smooth start-up and slow-down, vital in reducing the chance of

disorientation of the crystal plates to a minimum. Maximum speed, acceleration, deceleration and jerk are programmed such that in a minimum of time and with maximum smoothness the next measurement position is reached.
The limit switches are used for calibration of the Lyot filter. After hitting a switch the motor rotates backwards until it finds the first index pulse. This gives an accurate zero-point. Precise calibration is done just before the observations by tuning through the H-alpha line and measuring the minimum intensity of a defocused image. During tuning the filter is always moved in one direction in order to avoid backlash in the gear train.

2.6 Tuning scheme

A standard single speckle burst of 100 images takes around 10 seconds (the typical exposure time is 20 ms for the slowest camera and the CCD readout time is 83 ms). A burst is split up into 5 different sub-bursts, each 20 frames long. Between two sub-bursts the Lyot filter is shifted in wavelength and all cameras are idle. The shift in wavelength between two successive points is typical 0.035 nm and takes 0.6 sec (maximum velocity 0.1 nm/sec, acceleration 0.8 nm/sec^2, jerk 0.64 nm/sec^3). The total burst length then sums up to 14 sec, taking into account that moving back to the initial position takes longer. For the continuum channels the 5 sub-bursts are summed up and treated as a single 100 frame speckle burst during speckle processing. For H-alpha every single sub-burst is reconstructed separately with help of the total burst made in the red continuum channel (using the Keller-von der Lühe method, see sub-section 2.1).
The schedule above is the standard DOT tuning schedule, but observers are free to choose other schedules (e.g. 3 or 7 sub-bursts).

3. DOT SPECKLE PROCESSOR

As mentioned in sub-section 1.2, per day 1.6 Terabyte can be stored on the local hard disks. Thirty percent of this represents H-alpha data. It is impracticable to archive such an amount day after day, and even the transfer to another location causes serious problems. Therefore the raw data should be reduced as fast as possible locally at the observatory. For this purpose a computer farm has been built, being a dedicated cluster consisting of 70 processors, known as DSP (DOT Speckle Processor). The DSP is able to reduce 1.6 Terabyte within 24 hours. The speckle reconstruction software has been rewritten in a parallel version and ported form IDL to C. Extensive tests on other parallel clusters demonstrated that the actual speckle reconstruction code parallelizes almost perfectly, although the pre- and post-processing were harder to parallelize.
A 1 Gigabit switch pipes the data stream through optical fibres to the location of the DSP, about 100 m away from the telescope. The DSP (Figure 6) consists of five modules, three of them having a master with a 1.2 Terabyte RAID array, and 12 computing nodes. The two other modules are identical, however without storage. In each module the master handles pre- and post-processing and shares out the speckle reconstruction per subfield to the 12 low-memory nodes. Every module reconstructs one or two wavelength channels, the two Lyot channels.
During the design of the DSP the heat production was a major issue. An innovative and new development is the direct cooling of the CPUs, memory controllers and voltage regulators with water. The coolers (manufactured by Atotech, Germany) use a micro-channel canal structure, leading to high efficiency. The big advantage of water cooling is the minimized overall heat production compared to air cooling (due to the much better heat transfer coefficient consequently a smaller climate control system is needed) and the achievable extremely compact housing (no need for big air flow channels). The 70 processors are housed on 35 boards and are built with the 15 hard disks into 2 racks of only 24HE. For the processors Intel Xeon 2.4 GHz CPUs were chosen after intensive research for the best ratio of computation power and power consumption.
The heat produced by the auxiliary electronics which couldn't be cooled with water is taken away with a small secondary air cooling system. The air is cooled against cold water from an active compressor cooling machine. The passive water system of the CPUs and the active water system of the auxiliary electronics transfer their heat to a third water circuit containing a plastic water tank of 5000 l where the warm water is stored. It avoids the release of heat during day and night when observations by solar- and nighttime telescopes take place. Release through a radiator with fan is done only during the early morning and late afternoon after sunrise and before sunset.
The chosen design is a new approach of heat release for computer systems near astronomical installations, although the total heat release is modest compared to other installations. The peak power for the computer is 10 kW, the peak heat release capacity of the radiator plus fan is 60 kW. Normal operation values are substantial lower, because the nodes are not continuous running with maximum load. The increase of the water temperature in the tank between the release

periods is at most 15˚C which is the case after data reduction of a full 6-camera 8-hour run at 30s cadence and which doesn't occur daily because of seeing limitations.
The complete DSP is connected to a UPS which provides the cluster with power for 14 minutes after a power cut or interruption, enough to safely stop the calculations and shut down all nodes. An essential part of the DSP is the control and safety software, which monitors the conditions of all nodes and automatically shuts nodes down in case of over-heating, problems with the cooling circuit and leakage. During start-up all nodes are switched on one-by-one in order to avoid the creation of power dips in the observatory 400V net. Now the cluster is in full operation, a look into the DOT data base shows immediately the increase in data output during last year. For the manufacturer (Icebear Systems GmbH, Münich, Germany) the DSP was a pilot project and has been used as test facility for extensive measurements to learn more about heat-transfer and -storage details.

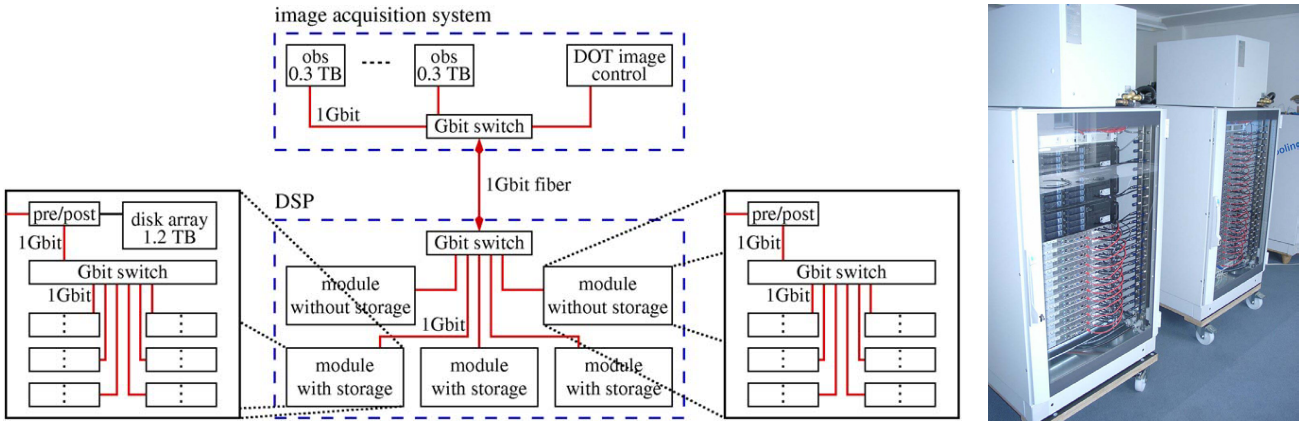

Fig. 6. DSP architecture: *(left)* the upper boxes (obs) denote the image-acquisition computers, one per camera. These together with the DOT image control workstation are located in the DOT observing room in the basement of the Swedish SST building. A 1 Gbit switch pipes the data stream through optical fibres to the DSP. The image acquisition system distributes the processing over five modules. The head node in each module handles the pre- and post-processing, and shares out the speckle reconstruction per subfield to 12 low-memory CPU's, two CPUs per board. Three of the five modules each have 1.2 Terabyte hard disks, so all together 3.6 TB is available for data storage sufficient for intermediate storage of two full observing days; *(right)* the complete DSP is housed in two 19" racks, 1.2m high.

4. RESULTS

By tuning the wavelength of the Lyot filter, the images collected with the camera move in altitude from the high chromosphere (at line center) to lower regions of the chromosphere in the line wings. The other channels image other regimes, ranging from the deep photosphere (G-band), via photosphere (blue & red continuum) to low chromosphere (Ca II H). Together they deliver an extended tomographic view of the solar atmosphere combining high-resolution, large-field, high-cadence and long-duration observations, which is nowadays a must in solar physics, as it becomes a science of movies showing all phenomena where magnetic topology plays a role. In this respect the DOT fills a solar physics niche and shares frequently in international multi-telescope campaigns combining many different diagnostics such as spectroscopy, Stokes vector polarimetry, Doppler mapping and EUV imaging from space [1, 20].
With the addition of the H-alpha channel the high-chromosphere is added which closes the gap between photosphere/ low chromosphere and processes in the corona. A particularly useful property of the H-alpha channel is that it provides in every image burst, as taken once per 15 seconds at maximum speed, not only a H-alpha line core image, but as well two wavelength positions in the blue wing and two in the red wing, plus a Dopplergram, all speckle reconstructed. Figure 1 shows a typical example of a speckle reconstructed DOT multi-channel image, taken in July, 2005 showing many different filtergrams, including H-alpha wing images and an H-alpha Dopplergram. Paper only permits to reproduce single images, but every picture printed is a snapshot of a movie, unveiling our sun's dynamical nature. It not only shows the evolution in time, but as a consequence of the fixed time cadence, DOT data are particularly well suited for frequency analysis. Figure 8 shows as an example oscillations in umbra and penumbra of a sunspot which do differ in frequency.

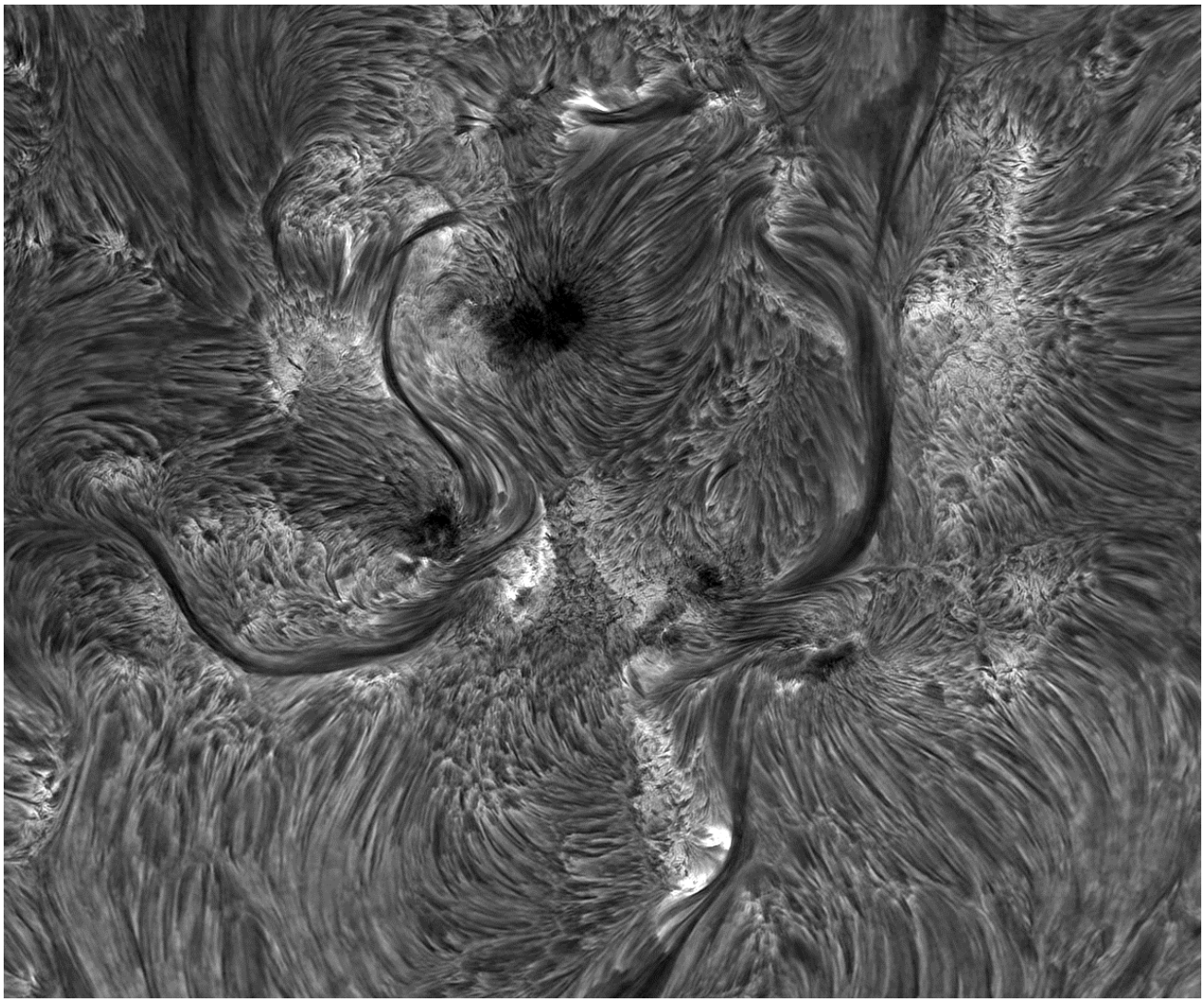

Fig. 7. 2x2 mosaic of DOT images in the H-alpha line core taken on June 8, 2005. The field measures 182 x 133 arcsec. The mosaic shows umbrae of the different sunspots which remain dark in H-alpha. So-called fibrils emanate away from the sunspots and they outline magnetic connections between different areas. The many fibrils show how complex solar magnetism is arranged. The bright areas surrounding the sunspots are plage, where large numbers of magnetic elements cluster together. The long slender dark structures are filaments. They end in bipolar regions where both positive and negative magnetic fields emerge through the solar surface.

A recent H-alpha result is shown in Figure 7, displaying a mosaic of several H-alpha images. The mosaic demonstrates at once how complex phenomena observed in the Balmer H-alpha line are. It combines intensity variations due to a change in temperature and velocity and shows structures on different heights due to the low density. For this reason full profile modeling has to be done and filtergrams are needed at a number of wavelength positions. The Balmer H-alpha line originates from the most abundant element and its high excitation energy causes this line to respond to gas at high temperatures. It maps fibrils in the transition zone between chromosphere and corona, typically at a height of a few thousand kilometers. Fibrils are obviously controlled by magnetic fields and many originate in the spot and in intergranular magnetic elements as visible in the G-band. The transition region has often been modeled as a spherical shell, however high-resolution H-alpha movies immediately show this is far too simple. H-alpha images show filaments and prominences, consisting of cool gas up and into the corona, long lasting features, full with MHD physics. Key research topics we like to address with help of the H-alpha data are related to the canopy transition: wave penetration and heating, moss structure and its dynamics, spicule physics and tube-loop coupling.

A first result is the study of bright intergranular magnetic elements in the blue wing of H-alpha, similar to the bright points in the G-band at 430.5 nm, but surprisingly showing a much higher contrast. From simulations it was found that they obey near LTE-line formation and are predominantly photospheric. The conclusion is that they represent a promising proxy magnetometer to locate and trace isolated magnetic elements with time [21].

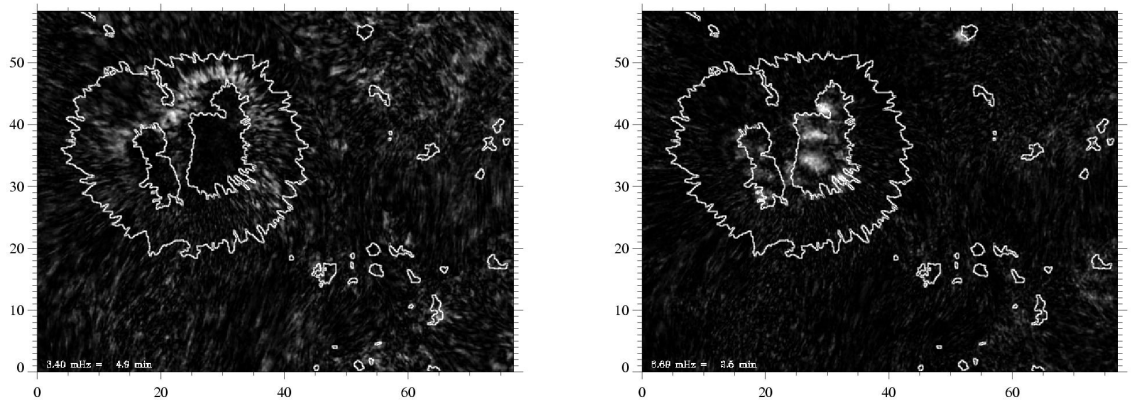

Fig. 8. Due to the fixed time steps between successive speckle bursts, the DOT is well suited for frequency analysis. Here dominant frequencies in a sunspot are shown (sunspots outlined with white contours) taken with the H-alpha channel on October 16, 2004. (*Left*) 3 minute oscillations; *(right)* 5-minute oscillations.

5. FUTURE DEVELOPMENTS

All DOT cameras are precisely co-aligned and have equal focal length. Due to the lower diffraction limit in the red part of the spectrum it is of advantage to de-magnify the H-alpha channel, giving away co-alignment, but gaining in field-size. Especially for H-alpha it is of advantage to have big field coverage which opens the way to track magnetic loops. A diffraction limited zoom lens has been designed, which could be used to trade-in resolution for field-size.
As a result of the small sub-bursts taken, the signal-to-noise ratio turns out to be a critical factor. It is of advantage to invest in new cameras with faster readout. A higher frame-rate provides for larger sub-bursts, which improves the speckle redundancy. A realistic option is to perform direct speckle on H-alpha and use the broad-band channel for co-alignment. We expect this will improve quality, especially on days with non-optimal conditions. Faster cameras create the possibility for higher burst cadences too, enabling the detection of faster phenomena: from the H-alpha sub-bursts we found that velocities easily exceed sound speed. A valuable option we can do already now is taking all sub-bursts at the same wavelength position. This delivers time series at a single H-alpha wavelength with 2 seconds time resolution.
The H-alpha channel should benefit from cameras with a wider dynamic range, the 10-bit of the current system is on the low end.
Currently the multi-wavelength imaging system of the DOT is being upgraded with a second Lyot-filter, built by Skomorovsky [13, 22] for the Ba II line (455.4 nm) and which can be operated in H-beta (486.1 nm) too. It will be equipped with a broad-band channel similar to the H-alpha channel described here and combined with a polarimeter [23].

ACKNOWLEDGEMENTS

The DOT is operated by Utrecht University at the Spanish Observatorio del Roque de los Muchachos of the Instituto de Astrofísica de Canarias and is presently funded by Utrecht University, the Netherlands Graduate School for Astronomy NOVA, the Netherlands Organization for Scientific Research NWO, and SOZOU. The DOT has been built by the Physics Instrumental Group of Utrecht University IGF and the Central Workshop of Delft University (now DEMO TU-Delft) with funding from Technology Foundation STW. The DOT Speckle Processor was a development of the Astronomical Institute and the Computational Physics Group both of the Department of Physics and Astronomy of the Utrecht University in cooperation with the Solar Physics group of the Institutt for Teoretisk Astrofysikk, Det Matematisk-Naturvitenskapelige Fakultet, Oslo University and Icebear Systems, HTP Microsystems, Atotech and Rittal, and part of the EC-TMR European Solar Magnetometry Network ESMN. It was funded by NWO and SOZOU. The

DOT team enjoys hospitality at the solar telescope building of the Royal Swedish Academy of Sciences. We thank Victor Gaizauskas and the National Research Council of Canada for making the H-alpha filter available for the DOT.

REFERENCES

1. R.J. Rutten, R.H. Hammerschlag, F.C.M. Bettonvil, P. Sütterlin, A.G. de Wijn, "DOT tomography of the solar atmosphere I. Telescope summary and program definition", A&A **413**, 1183, 2004.
2. R.H. Hammerschlag, "Construction Outlines of the Utrecht Open Solar Telescope*", Solar Instrumentation: What's next?*, R.B. Dunn, pp. 547-582, Sacramento Peak National Observatory, Sunspot, 1981.
3. F.C.M. Bettonvil, R.H. Hammerschlag, P. Sütterlin, A.P.L. Jägers, R.J. Rutten, "Multi-wavelength imaging system for the Dutch Open Telescope", *SPIE* Vol. 4853, pp. 306-317, 2002.
4. R.H. Hammerschlag, "Excursion: Tower, Parking Lot, Geostationary Orbit*", Solar Instrumentation: What's next?*, R.B. Dunn, pp. 583-599, Sacramento Peak National Observatory, Sunspot, 1981.
5. R.J. Rutten, A.G. de Wijn, P. Sütterlin, F.C.M. Bettonvil, R.H. Hammerschlag, "Opening the Dutch Open Telescope", *Magnetic Coupling of the Solar Atmosphere*, Procs. Euroconference/IAU Colloq. 188, pp. 565, ESA SP-505, 2002.
6. R.H. Hammerschlag, "A telescope drive with emphasis on stability", *SPIE* Vol. 444, pp.138-146, 1983.
7. R. Volkmer, O. von der Lühe, F. Kneer, J. Staude, T. Berkefeld, A. Hofmann, W. Schmidt, M. Sobotka, D. Soltau, E. Whier, A. Wittmann, "GREGOR, the new 1.5 m solar telescope on Tenerife", *SPIE* Vol. 4853, pp. 360-369, 2002.
8. S.L. Keil, T. Rimmele, C. Keller, F. Hill, R. Radick, J. Oschmann, M. Warner, N. Dalrymple, J. Briggs, S. Hegwer, D. Ren, "Design and development of the Advanced Technology Solar Telescope", *SPIE* Vol. 4853, pp. 240-251, 2002.
9. F.C.M. Bettonvil, R.H. Hammerschlag, P. Sütterlin, R.J. Rutten, A.P.L. Jägers, F. Snik, "DOT++: The Dutch Open Telescope with 1.4-m aperture", *SPIE* Vol.5489, pp. 362, 2004
10. R.H. Hammerschlag, O. von der Lühe, F.C.M. Bettonvil, A.P.L. Jägers, F. Snik, „GISOT: A giant solar telescope", *SPIE* Vol. 5489, pp. 491, 2004.
11. R.H. Hammerschlag, A.P.L. Jägers, F.C.M. Bettonvil, "Large Open Telescope: Size-upscaling from DOT to LOT", *SPIE* Vol. 4853, pp. 294-305, 2002.
12. R.H. Hammerschlag, F.C.M. Bettonvil, A.P.L. Jägers, "Towers for Telescopes with extreme stability: active or passive?", *SPIE* Vol. 6273, paper 61, 2006.
13. P. Sütterlin, R.H. Hammerschlag, F.C.M. Bettonvil, R.J. Rutten, V.I. Skomorovsky, G.N. Domyshev, "A multi-Channel Speckle Imaging System for the DOT", *Advanced Solar Polarimetry – Theory, Observation, and Instrumentation*, M. Sigwarth, Procs. 20th NSO/SP Summer Workshop, ASP Conf. Ser. 236, pp. 431, 2001.
14. C.U. Keller, O. von der Lühe, "Solar speckle interferometry", A&A **261**, pp. 321, 1992.
15. B. Lyot, "Un monochromateur à grand champ utilisant les interferences en lumière polarisée", Compt. Rend. Acad Sci. **197**, 1593, 1933.
16. B. Lyot, "Le filtre monochromatique polarisant et ses applications en physique solaire", Ann. Astrophys. **7**, No. 1-2, 31, 1944.
17. J.W. Evans, "The Birefringent Filter", JOSA **39**, 229, 1949.
18. G.A. Gary, K.S. Balasubramaniam, "Additional Notes on the Selection of Multiple-Etalon System for ATST*", ATST Project Documentation Technical Note*, #0027, June 2004.
19. V. Gaizauskas, "The Ottawa River Solar Observatory ", JRAS Can. **70**, 1, 1976.
20. R.J. Rutten, "DOT Strategies versus Orbiter Strategies", *Solar Encounter: the first Solar Orbiter workshop*, A. Wilson, pp. 357, Tenerife, ESA SP-493, 2001.
21. J. Leenaarts, R.J. Rutten, P. Sütterlin, M. Carlsson, H. Uitenbroek, "DOT tomography of the solar atmosphere VI. Magnetic elements as bright points in the blue wing of Hα", A&A **449**, pp. 1209-1218, 2006.
22. G.I. Kushtal, V.I. Skomorovsky, "Advance of the geometrical measurements of the birefringent filter's crystal plates and two-dimensional measurements of Doppler velocity in the solar atmosphere", *SPIE* Vol. 4900, pp. 504, 2002.
23. F. Snik, F.C.M. Bettonvil, A.P.L. Jägers, R.H. Hammerschlag, R.J. Rutten, C.U. Keller, "The Ba II 4554 / Hβ imaging polarimeter for the Dutch Open Telescope", *Procs. 4th Solar Polarization Workshop*, ASP Conf. Ser., in press, 2006.